

Importance of the advection scheme for the simulation of water isotopes over Antarctica by atmospheric general circulation models: a case study for present-day and Last Glacial Maximum with LMDZ-iso

A. Cauquoin^{a,*}, C. Risi^b, É. Vignon^c

^aAlfred Wegener Institute, Helmholtz Centre for Polar and Marine Sciences, Bremerhaven, Germany

^bLaboratoire de Météorologie Dynamique/Institut Pierre-Simon Laplace (LMD/IPSL), CNRS, Sorbonne Universités, UPMC Univ Paris 06, Paris, France

^cEnvironmental Remote Sensing Laboratory (LTE), École Polytechnique Fédérale de Lausanne (EPFL), Lausanne, Switzerland

Abstract

Atmospheric general circulation models (AGCMs) are known to have a warm and isotopically enriched bias over Antarctica. We test here the hypothesis that these biases are partly consequences of a too diffusive advection. Exploiting the LMDZ-iso model, we show that a less diffusive representation of the advection, especially on the horizontal, is very important to reduce the bias in the isotopic contents of precipitation above this area. The choice of an appropriate representation of the advection is thus essential when using GCMs for paleoclimate applications based on polar water isotopes. Too much diffusive mixing along the poleward transport leads to overestimated isotopic contents in water vapor because dehydration by mixing follows a more enriched path than dehydration by Rayleigh distillation. The near-air surface temperature is also influenced, to a lesser extent, by the diffusive properties of the advection scheme directly via the advection of the air and indirectly via the radiative effects of changes in high cloud fraction and water vapor. A too diffusive horizontal advection increases the temperature and so also contributes to enrich the isotopic contents of water vapor over Antarctica through a reduction of the distillation. The temporal relationship, from Last Glacial Maximum (LGM) to present-day conditions, between the mean annual near-air surface temperature and the water isotopic contents of precipitation for a specific location can also be impacted, with significant consequences on the paleo-temperature reconstruction from observed changes in water isotopes.

Keywords: water stable isotopes, Antarctica, AGCM, advection, isotope-temperature gradient.

1. Introduction

Water stable isotopologues (hereafter designated by the term “water isotopes”), are integrated tracers of the water cycle. Especially, the isotopic composition recorded in polar ice cores enabled the reconstruction of past temperature variations (Jouzel, 2013, and references therein). For example, low accumulation sites that are typical on the East Antarctic Plateau (< 10 cm water-equivalent yr^{-1}) provided the longest ice core records, making it pos-

sible to reconstruct past climate over several glacial-interglacial cycles (Jouzel et al., 2007). However, the interpretation of isotope signals remains challenging because of the numerous and complex processes involved (water vapor transport, fractionation during the phase changes in the water cycle, distillation effect...). This is particularly the case for Antarctica because this part of the world is subject to extreme weather conditions.

To improve our knowledge on the mechanisms controlling the water isotopes distribution, atmospheric general circulation models (AGCMs) enhanced by the capability to explicitly simulate the hydrological cycle of the water isotopes (H_2^{16}O , HDO , H_2^{17}O , H_2^{18}O) are now frequently used

*Corresponding author

Email address: alexandre.cauquoin@awi.de (A. Cauquoin)

(Joussaume et al., 1984; Risi et al., 2010b; Werner et al., 2011). Water isotopes in climate models have been used, for example, to better understand how the climatic signal is recorded by isotopes in polar ice cores at paleoclimatic time scales (Werner et al., 2001).

However, some issues remain concerning the simulation of the climate over the Antarctic continent by AGCMs. For example, they frequently present a near-surface warm bias over this area (Masson-Delmotte et al., 2006) and isotopic values in precipitation that are not depleted enough compared to observations (Lee et al., 2007; Risi et al., 2010b; Werner et al., 2011). This raises the question why many of the AGCMs have these warm and enriched in heavy water isotopes biases over Antarctica.

In this paper, we hypothesize that one part of these biases is associated with an excessively diffusive water vapor transport, i.e. transport that is associated with too much mixing. According to previous studies, the diffusive properties of the advection scheme in the AGCMs, on the horizontal as well on the vertical, can have an impact on the simulation of humidity and of its water isotope contents. On the horizontal, dehydration of air masses by mixing with a drier air mass leads to more enriched water vapor than dehydration by condensation and associated Rayleigh distillation (Galewsky and Hurley, 2010). For the same reason, poleward water vapor transport by eddies (which act as mixing) leads to more enriched water vapor in Antarctica than transport by steady advection (Hendricks et al., 2000). On the vertical, the excessive diffusion during water vapor transport seems to be the cause of the moist bias found in most AGCMs in the tropical and subtropical mid and upper troposphere, and of the poor simulation of isotopic seasonality in the subtropics (Risi et al., 2012). The diffusivity of the advection scheme in the vertical has also important consequences on modeling of tracers like tritium by affecting greatly its residence time in the stratosphere, and so its downward transport from the stratosphere to the troposphere (Cauquoin et al., 2016).

The goal of this paper is to test whether the warm and enriched biases in Antarctica are associated with an excessively diffusive water vapor transport, both on the horizontal and on the vertical. The diffusive character of the advection can be varied by modifying either the advection scheme or the resolution of the simulation, and we test both possibilities. Finally, we explore if a too diffusive water

vapor transport can affect the temporal water isotopes – temperature slope between the Last Glacial Maximum (LGM, 21 ka) and present-day periods.

2. Model, simulations and data

2.1. Model and simulations

We use here the isotopic AGCM LMDZ-iso (Risi et al., 2010b) at a standard latitude-longitude R96 grid resolution ($2.5^\circ \times 3.75^\circ$), and with 39 layers in the vertical spread in a way to ensure a realistic description of the stratosphere and of the Brewer-Dobson circulation (Lott et al., 2005). Water isotopes are implemented in a way similar to other state-of-the-art isotope-enabled AGCM (Risi et al., 2010b). The isotopic composition of glaciers R_{glacier} is calculated prognostically in the model. It is a precipitation-weighted average of the previous snow fall. At each time step and in each grid box, it is updated as:

$$R_{\text{glacier}}(t + dt) = \frac{h_{\text{glacier}} \times R_{\text{glacier}}(t) + iso_{\text{snowfall}} \times dt}{h_{\text{glacier}} + H_2O_{\text{snowfall}} \times dt} \quad (1)$$

with $h_{\text{glacier}} = 20 \text{ kg.m}^{-2}$ the height scale for the glacier, iso_{snowfall} and H_2O_{snowfall} the snowfall of isotopes and standard water in $\text{kg.m}^{-2}.\text{s}^{-1}$ and $dt = 30 \times 60 \text{ s}$. No fractionation is assumed during the runoff and sublimation of glaciers ice. The model has been validated at global scale for the simulation of both atmospheric (Hourdin et al., 2006) and isotopic (Risi et al., 2010b) variables, and has been extensively compared to various isotopic measurements in polar regions (Casado et al., 2013; Steen-Larsen et al., 2013, 2014, 2017; Bonne et al., 2014, 2015; Touzeau et al., 2016; Ritter et al., 2016; Stenni et al., 2016). LMDZ-iso is also able to simulate the H_2^{17}O distribution (Risi et al., 2013) but we do not consider it here because the limitations inherent to the AGCMs lead to strong uncertainties and numerical errors on the spatio-temporal distribution of this isotope. 2 years of spin-up have been performed for all the simulations presented hereafter.

To quantify the effects of the prescribed advection scheme on water stable isotope values over Antarctica, we first performed three sensitivity simulations with LMDZ-iso under present-day conditions for the post spin-up period 1990-2008 (i.e. 19 model years), following the model setup from

(Cauquoin et al., 2016) i.e. simulations follow the AMIP protocol (Gates, 1992), forced by monthly observed sea-surface temperatures and nudged by the horizontal winds from 20CR reanalyses (Compo et al., 2011): (1) one control simulation with the van Leer (1977) advection scheme (called VL), which is a second order monotonic finite volume scheme prescribed by default in the standard version of the model (Risi et al., 2010b); and two other simulations whose the van Leer advection scheme has been replaced by a single upstream scheme (Godunov, 1959) on (2) the horizontal plane (UP_xy) and on (3) the vertical direction (UP_z). Depending on one tunable parameter, the LMDZ model can be used with these 2 versions of the advection scheme according to the object of study (Risi et al., 2012). The advection scheme in the simulations presented in the LMDZ-iso reference paper from Risi et al. (2010b) was set erroneously to the simple upstream scheme rather than to the van Leer’s scheme (Risi et al., 2010a), and has little influence on their simulated spatial and temporal distributions of water isotopes at a global scale. However, as we will show here, this has considerable effect on the spatial distribution of these proxies over region with extreme weather conditions such as Antarctica. The 2-year spin-up time is enough to reach equilibrium. In the VL simulation, the globally and annually average values of temperature and $\delta^{18}\text{O}$ in precipitation for 1990 are 13.06°C and -7.53‰ respectively, very close to the average values over the whole period 1990–2008 (13.14°C and -7.57‰) within the average interannual variability of 0.15°C and 0.06‰ . The conclusion is the same if we focus on the 60°S – 90°S area instead: the average values of temperature and $\delta^{18}\text{O}$ in precipitation for the year 1990 are -17.89°C and -25.45‰ respectively, very close to the average values over the whole period 1990–2008 (-17.71°C and -25.34‰) within the average interannual variability of 0.43°C and 0.29‰ .

The detailed description of the mixing ratio by the van Leer’s (1977) scheme and its comparison with the upstream scheme (Godunov, 1959) can be found in the Appendix A of Cauquoin et al. (2016). To resume, the mixing ratio at the left boundary of box i , $q_{i-1/2}$, is calculated as a linear combination of the mixing ratio in the boxes $i-1$ and i in the van Leer’s scheme whereas in the upstream scheme $q_{i-1/2} = q_{i-1}$. This means that in the upstream scheme, even if the air mass flux from grid box $i-1$ to grid box i is very small, the air that is advected into box i has the same water vapor mixing ratio as

grid box $i-1$ as a whole. This makes the upstream scheme much more diffusive. An example of the effect of these 2 different advection schemes in a very idealized case is given in the figure 3 (top panel) of Hourdin and Armengaud (1999). In a single dimension case, a tracer distribution is initially rectangle and is advected with a constant velocity such that Courant number is equal to 0.2. After 70 iterations, the initial rectangle shape is almost unchanged with the van Leer scheme, whereas it spreads into a flat Gaussian shape with the upstream scheme. Quantitatively, almost half of the tracer mass becomes outside the initial rectangle shape with the upstream scheme.

Increasing the grid resolution is equivalent to using an advection scheme that is less diffusive. Indeed, these finite-difference schemes are discretization methods and so depend on the chosen spatial resolution. To check that our findings and conclusions are consistent, we performed two more UP_xy and VL simulations under present-day conditions with the same configuration as presented above but at the R144 resolution (latitude-longitude grid resolution of $1.27^\circ \times 2.5^\circ$).

Finally, we evaluate the impacts of applying advection schemes with different diffusive properties on the temporal relationship between water isotopic contents of precipitation and mean air surface temperature, essential for paleo-temperature reconstructions. For this, we effected 12 years long (the two first years being used for the spin-up) UP_xy and VL simulations for present-day “free” (i.e. not nudged by the 20CR reanalyses, still following the AMIP protocol) and LGM conditions at the R96 resolution. For the LGM simulations, the PMIP3 protocol is applied (Braconnot et al., 2012). Orbital parameters and greenhouse gas concentrations are set to their LGM values. ICE-5G ice sheet conditions are applied (Peltier, 1994). LMDZ-iso is forced by the climatological sea-surface temperatures (SSTs) and sea ice from the IPSL-CM4 model (Marti et al., 2005). The SST simulated by IPSL-CM4 for pre-industrial conditions (PI) has a global bias of -0.95 Kelvin with a cold bias in the mid-latitudes, a warm bias on the eastern side of the tropical oceans and on the Southern Ocean, and a particularly strong cold bias in the North Atlantic (Hourdin et al., 2013). To avoid confusing these biases with LGM – present-day signals, we use the SSTs from an IPSL PI simulation in the following way to cancel out the biases in the IPSL model common to both the LGM and PI simula-

tions (see details in Risi et al. (2010b)): $SST_{\text{forcing}} = SST_{\text{LGM}} - SST_{\text{PI}} + SST_{\text{AMIP}}$. We set the sea surface $\delta^{18}\text{O}$ to $+1.2\text{‰}$ and assume no glacial change in the mean deuterium excess in the ocean, as in Risi et al. (2010b). Note once again that the 2-year spin-up time is enough to reach equilibrium. In the VL present-day “free” simulation, the globally and annually averaged values of temperature and $\delta^{18}\text{O}$ in precipitation for the first post spin-up model year are 12.54°C and -8.27‰ respectively, very close to the average values over the 10 years of simulation (12.54°C and -8.34‰) in comparison to the interannual variabilities of 0.06°C and 0.06‰ . The conclusion still holds if we focus on the 60°S – 90°S area instead: the average values of temperature and $\delta^{18}\text{O}$ in precipitation for the first post spin-up year are -22.03°C and -26.08‰ respectively, very close to the average values over the 10 years of simulation (-22.04°C and -26.04‰) within the average interannual variability of 0.10°C and 0.21‰ .

We express the isotopic composition of difference water bodies in the usual δ -notation as the deviation from the Vienna Standard Mean Ocean Water (V-SMOW). So for H_2^{18}O , the $\delta^{18}\text{O}$ value is calculated as $\delta^{18}\text{O} = (([\text{H}_2^{18}\text{O}]/[\text{H}_2^{16}\text{O}])_{\text{sample}} / ([\text{H}_2^{18}\text{O}]/[\text{H}_2^{16}\text{O}]_{\text{V-SMOW}} - 1) \times 1000$. Long-time mean δ values are then calculated as precipitation-weighted mean. For the quantitative model-data comparisons, we retrieve the model values at data geographical coordinates by bilinear interpolation. Without such an interpolation, i.e. considering the nearest grid point instead, the root-mean-squared errors (RMSE) of mean $\delta^{18}\text{O}$ and temperature from the VL simulation differ only by 0.5‰ and 0.14°C compared to the results presented below, so the uncertainty associated with the model-data co-location is small.

2.2. Observations

To analyze the model performance over Antarctica under present-day conditions, we make use of the observational isotope database compiled by Masson-Delmotte et al. (2008). We also focus especially on the East Antarctic plateau (defined by the black bold contour of 2500 m above sea level elevation in Figure 1) because this area provides the main reconstructions of past climate based on the interpretation of water stable isotope records. To compare the model-data agreement of our simulations with van Leer and upstream advection schemes for atmospheric boundary layer, inversion

temperatures, we use additional datasets for the EPICA Dome C station (EDC: $[75.10^\circ\text{S}; 123.35^\circ\text{E}]$): the surface temperature, the 10m-temperature and the downward longwave radiative flux at the surface (LW_{dn}) over the period 2011–2018 thanks to the CALVA program and the Baseline Surface Radiation Network (BRN) (Vignon et al., 2018, and references therein); and the observed precipitable water from radiosoundings data for the period 2010–2017. We are aware that the observations periods are not the same than our model period (1990–2008), giving a possible bias in the model-data comparison. For the cloud cover, we use the CALIPSO–GOCCP observations (Chepfer et al., 2010) over the period 2007–2008. We compare these data with the high-level cloud fraction over EDC simulated by LMDZ-iso through the COSP package (Bodas-Salcedo et al., 2011), which allows to simulate what the CALIOP instrument on-board CALIPSO would measure if it was into orbit above the simulated atmosphere.

3. Results and discussion

3.1. Model-data comparison for present-day conditions

3.1.1. Water stable isotopes

Figure 1 shows the observed annual mean $\delta^{18}\text{O}$ values in the snow surface in Antarctica compiled by Masson-Delmotte et al. (2008) (Figure 1a) and the difference with the modeled annual $\delta^{18}\text{O}$ in precipitation from the UP_z (Figure 1b), UP_xy (Figure 1c) and VL (Figure 1d) simulations. The spatial average over the 60°S – 90°S area of standard deviations of long-time $\delta^{18}\text{O}$ and δD model values is of 0.97 and 7.48 ‰, respectively. The results from the VL simulation are in better agreement with the $\delta^{18}\text{O}$ observations over Antarctica (Figure 1d). This is confirmed by the smaller root-mean-squared error of modeled $\delta^{18}\text{O}$ in precipitation from the VL simulation, calculated as the difference between the observed annual mean values and the LMDZ-iso results ($\text{RMSE} = 4.47\text{‰}$, i.e. 12.2 % of the observed mean Antarctic $\delta^{18}\text{O}$ value). The results from the VL simulation for the other isotopic variable δD is also the closest of the observations with a RMSE of 40.93 ‰ (Table 1, red background). Our simulated $\delta^{18}\text{O}$ in precipitation is very sensitive to the choice of the advection scheme on the horizontal plane, with more enriched values when a more diffusive

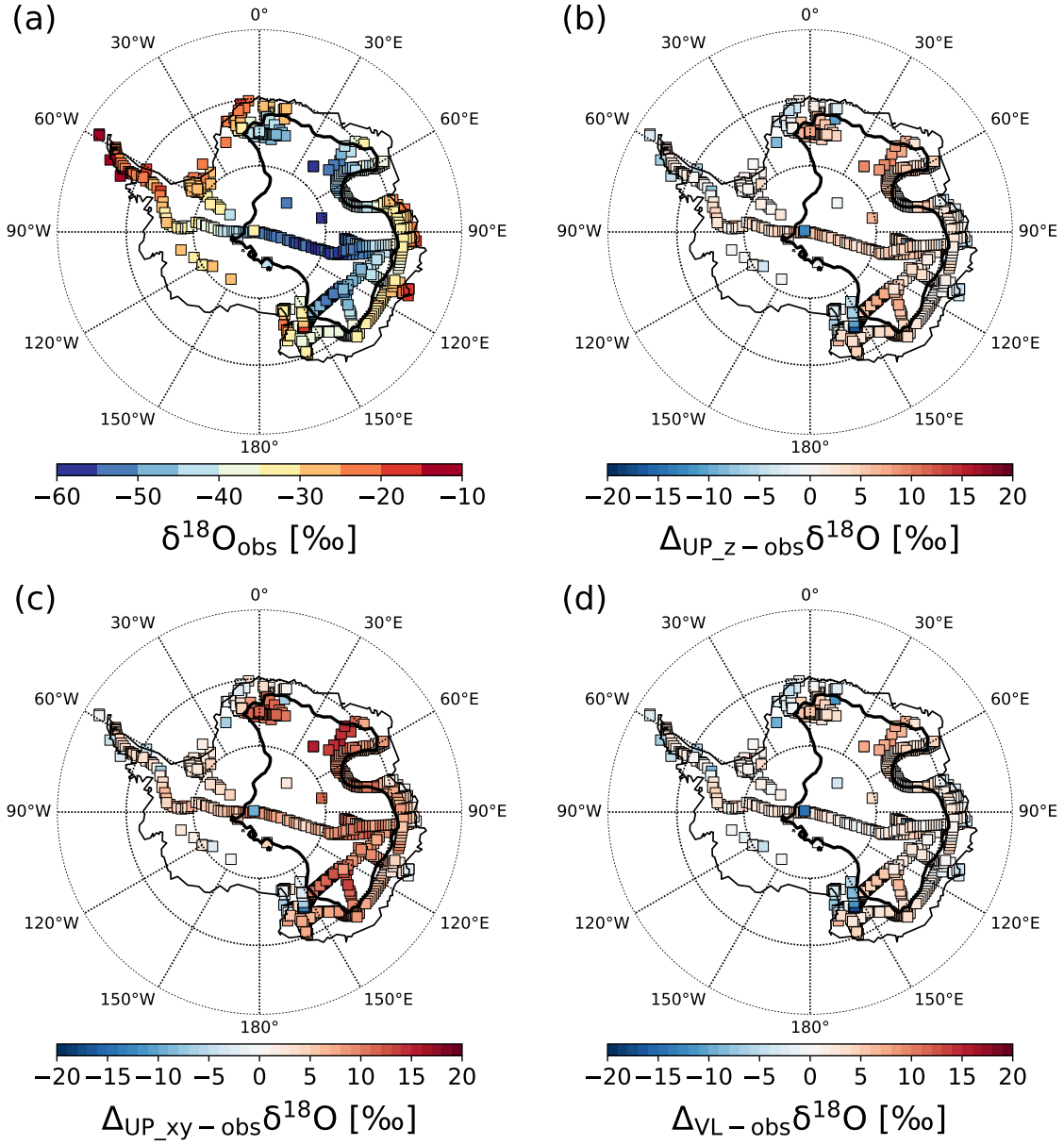


Figure 1: Map of Antarctica showing (a) the observed $\delta^{18}\text{O}$ values from the compilation by Masson-Delmotte et al. (2008), (b) the difference between the simulated $\delta^{18}\text{O}$ in precipitation and the $\delta^{18}\text{O}$ observations for the UP_z, (c) UP_{xy} and (d) VL simulations. The bold black line shows the contour of 2500 m above sea level elevation.

advection scheme is applied (Figure 1c). This is reflected by the mean $\delta^{18}\text{O}$ model value and RMSE, higher by 3.16 and 4.31 ‰ than the VL simulation values. On the contrary, the sensitivity of Antarctic $\delta^{18}\text{O}$ values to the diffusive properties of vertical advection is weak (Figure 1b) with an RMSE very close of the VL one (4.84 ‰). The results from the VL simulation for the other isotopic variable δD is also the closest of the observations with a RMSE of 40.93 ‰ (Table 1, red background). According to the observations, the East Antarctic plateau is where the water isotope values are the lowest (mean $\delta^{18}\text{O}$ below -40 ‰, Figure 1a) due to the very low temperatures. Because of the extreme cold and dry conditions at this area, one can see that the main disagreements between model outputs and observations are located at this place (Figure 1 and blue background of Table 1). Again, the isotopic outputs from the VL simulation are in better agreement with the observations (Table 1, blue background). These first results confirm that an excessively diffusive water vapor transport influences significantly the simulated isotopic and temperature values over Antarctica.

3.1.2. Temperature

The bias in temperature is deteriorated about in the same way when applying a more diffusive advection on the vertical direction or on the horizontal plane, as shown with the RMSE of annual mean temperature of 7.50, 7.31 and 6.60°C for the UP_z, UP_xy and VL simulations respectively (Table 1, red background). This tendency is the same when focusing on the East Antarctic plateau. However, in average over the East Antarctic plateau, the temperatures of -30.51 , -30.69 and -31.54 °C from the UP_z, UP_xy and VL simulations are all within the spatial average of standard deviations of long-time temperature values (0.87°C). These values are all much warmer than the average observed temperature (-36.93 °C). This shows that other factors than advection are responsible for the warm bias.

It has been suggested that the Antarctic warm bias in AGCMs could be linked to the general poor representation of the polar atmospheric boundary layer and related atmospheric inversion temperatures in these models (Krinner et al., 1997). Cesana and Chepfer (2012) have also shown that CMIP5 models generate too many high-level clouds (i.e. above an altitude of 6.72 km), that can partly explain the overestimation of temperatures in Antarctica, due to their effect on downwelling longwave

radiation. To go further, we compare the seasonal signals of surface temperature, near-surface thermal inversion (defined here as the difference between the 10m-temperature and the surface temperature), downward longwave radiative flux at the surface (LW_{dn}), integrated water vapor column and high cloud fraction at EDC from VL and UP_xy simulations with meteorological observations (see Figure 2 and the description of the data in section 2.2). The difference in LW_{dn} between the simulations VL and UP_xy at EDC is also present all over the East Antarctic plateau, confirming that EDC is representative of this area.

Both VL and UP_xy simulations have a warm bias at the surface (Figure 2a) and underestimate the near-surface inversion (Figure 2b), especially during the austral winter. This is mostly explained by an overly active turbulent mixing within stable boundary layers in LMDZ5 (Vignon et al., 2017). The disagreement with the observed near-surface inversion at EDC is exacerbated in the UP_xy simulation because the modeled surface temperature is more affected by the change of advection scheme than the modeled 10m-temperature. This is consistent with a higher total LW_{dn} flux over EDC in the UP_xy simulation than in the VL one (Figure 2c), by around 5 W.m^{-2} in summer and 8 W.m^{-2} in austral winter. The difference of LW_{dn} between our two simulations can be due to two aspects: the fraction of high cloud and the amount of water vapor (e.g., Vignon et al. (2018)). The modeled high-level cloud fraction over EDC for the period 2007–2008 is overestimated compared to the CALIPSO–GOCCP observations (Figure 2f). This finding is consistent with the results from Cesana and Chepfer (2012) for CMIP5 models and with Lacour et al. (2018) for dry areas over Greenland. This result also concurs with an overestimated relative humidity with respect to ice in the troposphere compared to radiosoundings (not shown) during winter seasons, especially in the UP_xy simulation. The disagreement of high cloud cover is clearly enhanced in the UP_xy case, which is consistent with stronger LW_{dn} in the UP_xy simulation. The comparison of LW_{dn} under clear sky in our two simulations (Figure 2d) can give us information about the contribution of cloud and water vapor on the variations of total LW_{dn} (Figure 2c). The stronger simulated LW_{dn} in the UP_xy simulation is due mainly to the high cloud in winter (70 %) and to both high cloud and water vapor during summer (42.5 and 57.5 %, respectively). The effect of water vapor on downward longwave radia-

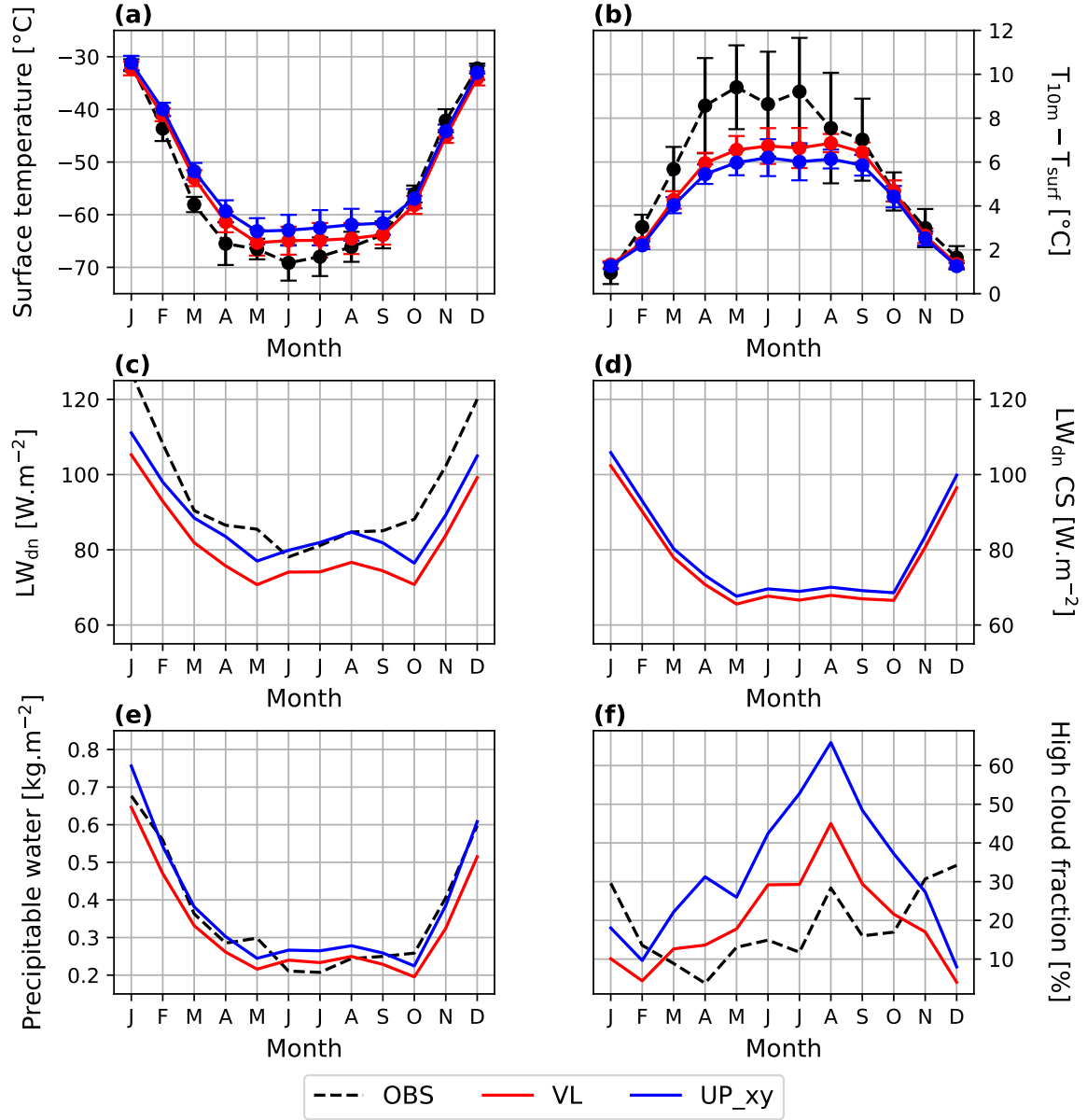


Figure 2: Multi-year monthly mean variations of (a) surface temperature, (b) near-surface thermal inversion (defined as the difference between the 10m-temperature and the surface temperature), (c and d) total and clear-sky component of downward longwave radiative flux at the surface, (e) precipitable water and (f) high cloud fraction above EPICA Dome C. The red and blue curves correspond to the VL and UP_xy simulation results, respectively. A comparison with observations (see section 2.2) is made when possible (dashed black lines).

Table 1: Observed and simulated annual mean values of temperature (T), $\delta^{18}\text{O}$ and δD for the full Antarctic dataset (red background) and restricted to the East-Antarctic plateau (blue background), and the corresponding RMSE.

	Mean data	Mean UP_z	RMSE UP_z	Mean UP_xy	RMSE UP_xy	Mean VL	RMSE VL
T ($^{\circ}\text{C}$)	-36.93	-30.51	7.50	-30.69	7.31	-31.54	6.60
$\delta^{18}\text{O}$ (‰)	-36.76	-34.85	4.84	-31.43	7.63	-35.74	4.47
δD (‰)	-289.62	-272.28	43.76	-251.34	62.00	-279.49	40.93
T ($^{\circ}\text{C}$)	-47.46	-39.49	8.38	-39.88	7.99	-40.71	7.23
$\delta^{18}\text{O}$ (‰)	-46.77	-42.27	5.03	-37.37	9.69	-43.76	3.80
δD (‰)	-366.98	-325.37	43.79	-291.99	76.44	-336.25	33.58

tive flux is also confirmed by the higher amount of precipitable water over EDC in the UP_xy simulation (Figure 2e). From these results, we deduce that the warmer surface temperature in the UP_xy simulation is due to the higher air temperature (direct effect of the horizontal upstream advection) and to the radiative amplification from high clouds and in a lesser extent from water vapor (indirect effect of the horizontal upstream advection).

The near-surface warm bias in LMDZ-iso, which is most pronounced for the coldest temperatures (see Figure 3), has the consequence that the distillation is not strong enough. Some microphysical processes and kinetic fractionation at very low temperature can be missed too. These different aspects could contribute to an overestimation of the $\delta^{18}\text{O}$ and δD in precipitation over Antarctica. Finally, the 20CR reanalysis assimilate only surface observations of air pressure and use the observed monthly sea surface temperature and sea ice concentration as lower boundary conditions. These less strong constraints, compared to other reanalyses, may cause biases on the surface temperature over the poles (A. Orsi, personal communication), that can impact our isotopic delta values.

3.1.3. Spatial $\delta^{18}\text{O}$ -temperature relationship

We compare now our simulated spatial $\delta^{18}\text{O}$ -temperature relationship and $\delta^{18}\text{O}$ values for a given temperature to those from the data compiled by Masson-Delmotte et al. (2008). Over the full temperature range, the spatial gradient is $0.83 \text{ ‰}^{\circ}\text{C}^{-1}$ in the VL simulation, very close of the observed one ($0.80 \text{ ‰}^{\circ}\text{C}^{-1}$). We make the same comparison but by restricting the dataset to the ones on the East Antarctic plateau (Figure 3). As noticed previously, the average modeled temperature over Antarctica is overestimated whatever the simulation considered. Especially, no simulated tem-

perature reaches a value below -50°C . Yet, simulated $\delta^{18}\text{O}$ values are too depleted for the temperature range between -49°C and -43.5°C . As a consequence, a steeper modeled $\delta^{18}\text{O}$ -temperature gradient is observed for the lowest temperatures, giving a modeled global gradient of $1.24 \text{ ‰}^{\circ}\text{C}^{-1}$ (thin orange line). If we restrict the fit to simulated temperatures higher than -43.5°C (vertical dashed line in Figure 3), corresponding to the change of slope in the simulated $\delta^{18}\text{O}$ -temperature relationship (thick orange line), the simulated gradient ($0.96 \text{ ‰}^{\circ}\text{C}^{-1}$) is in more reasonable agreement with the one from the observations ($0.85 \text{ ‰}^{\circ}\text{C}^{-1}$).

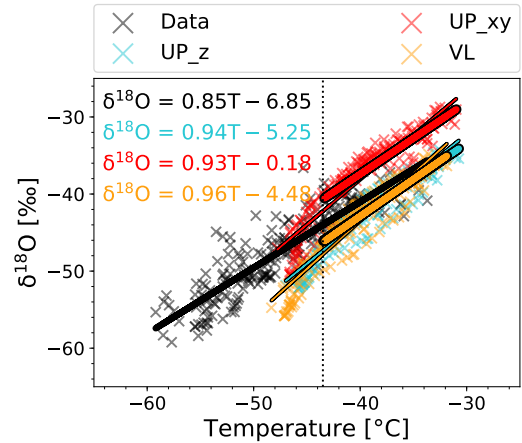


Figure 3: Relationship between $\delta^{18}\text{O}$ and temperature on the East-Antarctic plateau according to the observations (black) and the UP_z (blue), UP_xy (red) and VL (orange) simulations. For each simulation outputs, two linear regressions have been conducted: one on the full East-Antarctic plateau dataset (thin lines) and one on the same dataset without the temperatures below -43.5°C (bold lines) indicated by the vertical dashed line. The corresponding formulas of these latter are also shown.

We now discuss possible reasons that could explain why the simulated $\delta^{18}\text{O}$ -temperature slope is

too steep at very low temperatures. First, it could be related to missing representation of fractionation during sublimation from the surface. As for all AGCMs equipped with water isotopes, fractionation at sublimation is not taken into account in LMDZ-iso. However, this effect would lead to further decrease of the water vapor $\delta^{18}\text{O}$ in polar region and hence contribute to an even steeper $\delta^{18}\text{O}$ –temperature slope at low temperature (hence further accentuate the mismatch). Second, the slope mismatch could be related to poorly represented kinetic fractionation. As in all the other models equipped with water isotopes, the parameterization of kinetic effect during vapor-to-solid condensation is represented empirically using a linear relationship between the supersaturation and the condensation temperature (Risi et al., 2010b). A modification of the temperature can thus induce some change in the $\delta^{18}\text{O}$ of the condensate, but this effect is of second order compared to the distillation effect explaining much of the slope between $\delta^{18}\text{O}$ and surface temperature. Third, the slope mismatch could be related to a poor representation of the atmospheric boundary layer and of its related inversion temperature (Krinner et al., 1997; Masson-Delmotte et al., 2006), as shown in the Figure 2. In LMDZ-iso, the warm bias in the simulated condensation temperature is smaller than that in the simulated surface temperature. Therefore, the water vapor masses continue to be distilled when moving away from the coast, while the cooling simulated at the surface from the coast to the remote region of the East Antarctic plateau is much less steep than in the reality.

3.2. Comparison of the different simulations

3.2.1. Effects of the diffusive properties of the advection scheme

We compare here the results from our different present-day simulations at a R96 grid resolution. The UP_z simulation (upstream vertical advection, Figure 1b) increases the bias a little in $\delta^{18}\text{O}$, but its results stay relatively close of the $\delta^{18}\text{O}$ values from the VL simulation, indicated by the similar average values that differ only by 0.89‰ for all Antarctica (Table 1) that is smaller than the mean of the 60° S – 90° S standard deviations. On the other hand, the $\delta^{18}\text{O}$ outputs from the UP_{xy} simulation (upstream horizontal advection, Figure 1c) display greater differences with the VL simulation ones, and so with the isotopic data, as revealed by

the mean UP_{xy} – VL difference in $\delta^{18}\text{O}$ of 4.31‰. This is even more significant when focusing on the East Antarctic plateau, with a model–data difference in $\delta^{18}\text{O}$ reaching 20‰ at some locations. The annual mean $\delta^{18}\text{O}$ and δD values from the UP_{xy} simulation are increased by 6.39‰ and 44.26‰ compared to the VL simulation average values, in less agreement with the observations as shown by their respective RMSE values (Table 1, blue background). It shows that the diffusive property of the advection scheme on the horizontal plane is essential to better model the water isotope distribution, especially over Antarctica. To go further, one can also compare the $\delta^{18}\text{O}$ values at a fixed temperature for the UP_{xy} and VL simulations (Figure 3, red and orange crosses respectively). The $\delta^{18}\text{O}$ in precipitation for a temperature of -32°C over the East Antarctic plateau is already smaller by 6.1‰ in the VL simulation. This very significant difference in initial $\delta^{18}\text{O}$ can be attributed to the proportion of mixing against distillation that affects the water vapor during its transport. This lends support to our hypothesis that too much diffusive mixing along the poleward transport leads to overestimated $\delta^{18}\text{O}$ because dehydration by mixing follows a more enriched path than dehydration by Rayleigh distillation (Hendricks et al., 2000; Galewsky and Hurley, 2010). We expect the relative contribution of mixing vs. distillation to have the largest impact on $\delta^{18}\text{O}$ at latitudes where eddies are the most active. This is probably why the $\delta^{18}\text{O}$ difference between the VL and UP_{xy} simulation becomes large in mid-latitudes, over the austral ocean before arriving at the Antarctica coast (not shown), hence the difference in “initial” $\delta^{18}\text{O}$ in Figure 3.

As noticed in section 3.1.2, all our simulations overestimate the average temperature in Antarctica and even more on the East Antarctic plateau. A more diffusive advection on the horizontal or on the vertical increases the mean temperature value by 0.85 and 1.03°C respectively compared to the VL result. To explain such an influence of the advection on the temperature over Antarctica, even secondary, one can hypothesize that the Antarctic continent is better isolated, and so colder, when the advection of the model is less diffusive. If we focus now on the link between the temperature and the $\delta^{18}\text{O}$ in precipitation over all the continent, the $\delta^{18}\text{O}$ –temperature gradients according to our different R96 simulations UP_z, UP_{xy} and VL are at 0.79, 0.69 and 0.83‰.°C⁻¹ respectively. The difference between the VL and UP_{xy} gradient shows an effect

Table 2: Comparison of the observed annual mean values of temperature (T), $\delta^{18}\text{O}$ and δD for the full Antarctic dataset with four different LMDZ-iso simulations, combining different horizontal resolutions (R96 and R144) and different advection schemes (UP_xy and VL).

	Mean data	Mean UP_xy R96	Mean VL R96	Mean UP_xy R144	Mean VL R144
T ($^{\circ}\text{C}$)	-36.93	-30.69	-31.54	-31.45	-32.10
$\delta^{18}\text{O}$ (‰)	-36.76	-31.43	-35.74	-33.85	-37.64
δD (‰)	-289.62	-251.34	-279.49	-267.17	-289.55

of diffusive properties of the large-scale transport on the distillation process. This difference between the modeled $\delta^{18}\text{O}$ -temperature gradients is reduced if we restrict to the temperature range above -43.5°C over the East Antarctic plateau, with gradients of 0.93 and $0.96 \text{ ‰}^{\circ}\text{C}^{-1}$ according to the UP_xy and VL simulations respectively (Figure 3, red and orange thick lines).

Since the simulated temperature difference between the UP_xy and VL simulations is in the error margin, i.e. less than 1°C , we do not expect that the temperature difference explains the difference in spatial slopes. Rather, the larger slope in simulation VL is due to the larger relative contribution of Rayleigh distillation compared to mixing.

3.2.2. Effects of the horizontal grid resolution

We test now the hypothesis that to increase the horizontal resolution is equivalent to using an advection scheme that is less diffusive. The Antarctica mean results are summarized in the Table 2. Compared to the UP_xy R96 simulation, the average value of $\delta^{18}\text{O}$ in precipitation is decreased by 4.31 ‰ when the advection scheme is improved (VL R96), and by 2.42 ‰ when the horizontal resolution is increased (UP_xy R144), in better agreement with the observations. The picture is the same for the δD outputs. The decrease of the mean modeled temperature values, smaller than the mean of the long-time standard deviations on the $60^{\circ}\text{S} - 90^{\circ}\text{S}$ area, is the same by changing the advection scheme or by increasing the resolution: by 0.85°C and 0.76°C respectively. The best results are reached by improving both the advection scheme and the horizontal resolution at the same time, with model-data differences in temperature and $\delta^{18}\text{O}$ of 4.83°C and 0.88 ‰ respectively. This confirms that an increase of the horizontal resolution plays the same role as an improvement in the representation of the advection scheme on its horizontal plane (Hourdin and Armengaud, 1999). It is worth mentioning that the improvement in model-

data agreement using a higher horizontal grid resolution is probably not only due to an improved representation of the advection in the model but, among others, to a better resolved Antarctic topography and near surface circulation. Our results are consistent with the study of Werner et al. (2011) that shows, for an increased horizontal resolution, a better agreement of the simulated isotopic delta values and of the water isotope-temperature gradient with the observations. The seasonality in modeled Antarctic temperature and precipitation, which influences the precipitation-weighted isotope values, is not altered by the change of advection scheme or horizontal grid resolution.

3.2.3. Effects on the LGM to present-day change in temperature

We evaluate now the effects of the diffusive properties of the advection scheme on the $\delta^{18}\text{O}$ -temperature temporal slope at different Antarctic locations between LGM and present-day. For this, we compare the VL and UP_xy LGM simulations with their present-day “free” counterparts (i.e. without nudging). Figure 4a shows VL simulated temporal slopes in $\delta^{18}\text{O}$ -temperature at each location as $\Delta\delta^{18}\text{O}/\Delta T$. Over East Antarctica, the simulated temporal slope becomes larger inland, going from near to $0 \text{ ‰}^{\circ}\text{C}^{-1}$ on the coast to $2 \text{ ‰}^{\circ}\text{C}^{-1}$ on the deep East Antarctic plateau. Over West Antarctica, the temporal slopes are more heterogeneous and show variations from 0.1 to $1 \text{ ‰}^{\circ}\text{C}^{-1}$. The slopes at WDC (Wais Divide Core, square symbol), Siple Dome (triangle symbol), Vostok (circle symbol) and EDC (cross symbol) are of 0.80, 0.66, 0.73 and $0.37 \text{ ‰}^{\circ}\text{C}^{-1}$ respectively (calculated by considering the 9 grid cells centered on each drill location). Figure 4b shows the differences between the UP_xy and VL simulated slopes. As the spatial slopes from the VL simulation are higher than the UP_xy one, it is expected that the LGM to present-day temporal slopes are larger in the VL simulation than in the UP_xy one because of

the colder temperatures and of the higher relative contribution of the Rayleigh distillation. This is the case on the western part of the continent where the UP_xy temporal slopes are smaller than the VL ones by up to $0.6 \text{ ‰} \cdot \text{°C}^{-1}$. On the East Antarctic plateau, the VL $\delta^{18}\text{O}$ –temperature slopes are larger between the longitudes 100° E and 140° E than in UP_xy as well. The slope values are smaller in VL than in UP_xy only over the center of the continent, which corresponds to the lowest simulated temperature values and so where the gradient between the $\delta^{18}\text{O}$ and temperature values is much steeper (see 2nd paragraph of section 3.1.3), especially for LGM conditions.

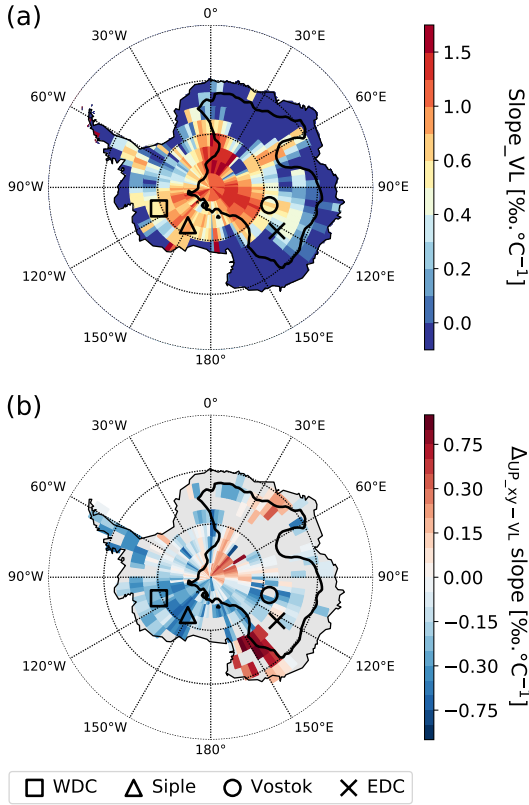


Figure 4: (a) Temporal slope ($\Delta\delta^{18}\text{O}/\Delta T$) between the present-day (PD) and LGM according to the VL simulations. (b) Difference with the temporal slope deduced from the UP_xy simulations. The grey areas indicate where the LGM–PD difference in $\delta^{18}\text{O}$ is lower than the standard deviation of the interannual variability. Square, triangle, circle and cross symbols represent the WDC, Siple Dome, Vostok and EDC sites respectively.

We highlight now the consequences that an excessively diffusive horizontal advection may have

on the LGM cooling reconstructed from simulated temporal slopes. For this, we calculated the difference in the LGM to present-day change in temperature deduced from the observed changes in $\delta^{18}\text{O}$ and simulated slopes ($\Delta\delta^{18}\text{O}/\Delta T$) by VL and UP_xy, at WDC and Siple Dome stations for West Antarctica, and Vostok and EDC stations for East Antarctica (Table 3). For WDC, Siple Dome and Vostok stations, the average changes in $\delta^{18}\text{O}$ between LGM and present-day are larger in the VL simulation, -11.98 , -9.88 and -3.90 ‰ respectively, than in the UP_xy simulation (-7.52 , -6.24 and -2.07 ‰ respectively). For the EDC station, the difference in LGM to present-day change in $\delta^{18}\text{O}$ between our VL and UP_xy simulations can be considered in the margin error (-1.97 and -1.70 ‰ for VL and UP_xy simulations respectively). The values deduced from the VL simulation are also in better agreement with the observations (Table 3). As previously noticed, the temporal $\delta^{18}\text{O}$ –temperature gradients at WDC, Siple Dome, Vostok and EDC are also larger in the VL simulation by 57 %, 65 %, 92 % and 26 % respectively, compared to the values deduced from the UP_xy simulation. As a consequence, if one applies the slope from the UP_xy simulation instead of the VL one, we would overestimate the present-day-to-LGM cooling at these stations by 4.34, 5.83, 3.76 and 2.95°C respectively. Even if the change in the temporal $\delta^{18}\text{O}$ –temperature gradient at EDC is relatively smaller than for the other stations, the consequence on the reconstructed present-day-to-LGM cooling value is still important. These results show that a more diffusive advection scheme on the horizontal plane can affect greatly the LGM to present-day temperature change deduced from observed $\delta^{18}\text{O}$ in precipitation.

4. Conclusions

We have tested with LMDZ-iso if the warm and isotopically enriched biases in Antarctica, frequently observed in the AGCMs, are associated with the diffusive property of the advection scheme. The simulated water isotope contents in Antarctica are very sensitive to the diffusive character of the water vapor transport on the horizontal plane. The higher the contribution of mixing (i.e. diffusion), the more enriched the precipitation. These findings are even more striking for the East Antarctic plateau where the main ice cores allowing paleoclimate reconstructions are located. Moreover,

Table 3: Sites of interest and their geographical coordinates, observed LGM to present-day changes in $\delta^{18}\text{O}$ (Wais Divide: WAIS Divide Project Members (2013), Schoenemann et al. (2014); Siple Dome: Brook et al. (2005), Schoenemann et al. (2014); Vostok: Vimeux et al. (2001), Landais et al. (2008, 2012); EDC: EPICA Comm. Members (2004), Stenni et al. (2010)), simulated LGM to present-day changes in $\delta^{18}\text{O}$ (UP_xy and VL simulations), simulated temporal $\delta^{18}\text{O}$ -temperature slopes and VL-UP_xy difference in reconstructed temperature change deduced from the observed $\delta^{18}\text{O}$ changes and the simulated temporal slopes. This difference is calculated as $-(\text{slope_UP_xy} - \text{slope_VL}) \times \Delta\delta^{18}\text{O}_{\text{obs}}/\text{slope_VL}^2$. Negative signs indicate that when using the UP_xy temporal slope, we overestimate the LGM cooling compared to using the VL temporal slope. The model values are based on the spatial averages over the 9 grid cells surrounding the ice cores geographical coordinates.

Site	Latitude	Longitude	LGM-PD $\delta^{18}\text{O}_{\text{obs}}$ (‰)	LGM-PD $\delta^{18}\text{O}_{\text{UP_xy}}$ (‰)	LGM-PD $\delta^{18}\text{O}_{\text{VL}}$ (‰)	Slope UP_xy (‰.°C ⁻¹)	Slope VL (‰.°C ⁻¹)	Difference in reconstructed ΔT (°C)
WDC	-79.47	-112.08	-9.44	-7.52	-11.98	0.51	0.80	-4.34
Siple Dome	-81.67	-148.82	-9.8	-6.24	-9.88	0.40	0.66	-5.83
Vostok	-78.47	106.87	-5.66	-2.07	-3.90	0.38	0.73	-3.76
EDC	-75.10	123.35	-6.74	-1.70	-1.97	0.31	0.37	-2.95

because the diffusive character of the large-scale transport influences the temperature in this region, even in a light way, this has an impact on the modeled water isotopic composition through the Rayleigh distillation. So, we conclude here that the excessive numerical diffusion has a large influence on the enriched isotopic bias. For the spatial isotope-temperature relationship over the East Antarctic plateau observed in LMDZ-iso, this latter is improved for the temperatures above -43.5°C , in more reasonable agreement with the observations. At the lowest temperatures (i.e. still over the East Antarctic plateau), that the model is not able to reach, the non-linearity observed in our simulations (the spatial $\delta^{18}\text{O}$ -temperature relationship is steeper for the lowest temperatures) can be unlikely explained at first order to missing or poorly represented kinetic fractionation. One can speculate that the water masses continue to be distilled when moving away from the coast, hence depleting the water vapor in heavy isotopes while the modeled temperature decrease from the coast to the remote region of the East Antarctic plateau is much less steep than in the reality. This more pronounced effect in the case of a more diffusive horizontal advection scheme could be due to the deteriorated representation of the inversion temperature. The temporal isotope-temperature relationship at some locations in Antarctica can be influenced by the diffusive properties of the advection scheme on its horizontal domain. As for the spatial gradient, an excessive numerical diffusion has the consequence to decrease the isotope-temperature temporal gradient, leading to a wrong estimation of the LGM to present-day temperature change deduced from observed $\delta^{18}\text{O}$. Our study demonstrates that a representation of the advection scheme in the AGCMs

taking into account water isotopes and isotopic gradients, especially on the horizontal domain, is an important step toward a more realistic modeling of water isotopes over Antarctica. Another way to improve this aspect is to increase the spatial resolution, which has the same effect as applying a less diffusive advection scheme on the water isotopic composition and the temperature. This study shows again the importance of using water stable isotopes in GCMs for the evaluation and quantification of the processes influencing the hydrological cycle, including the advection of water vapor. We expect our main results (excessive diffusive advection leading to warmer temperatures, moister boundary layer and more enriched water vapor) to be robust and to hold in other models as well. However, the quantitative response to the advection scheme may be modulated by the representation of boundary layer processes and high-cloud microphysics in each model.

Acknowledgements

We thank A. Landais for her useful suggestions on this manuscript, J.-B. Madeleine and C. Genthon for their kind support about inversion temperatures over EDC, and R. Guzman, C. Listowski and H. Chepfer for their help with the GOCCP data. This work was granted access to the HPC resources of IDRIS under the allocation 0292 made by GENCI. The research leading to these results has received funding from the European Research Council under the European Union's Seventh Framework Programme (FP7/20072013)/ERC grant agreement no. 30604. We thank Christophe Genthon and the CALVA program for acquiring and distributing meteorological data at Dome

C (<http://www.lmd.jussieu.fr/~cgenthon/SiteCALVA/CalvaBackground.html>) with the support of the french polar institute (IPEV). We also acknowledge the WCRP-BSRN network and Angelo Lupi for the dissemination of radiation data. Radiosoundings data at Dome C are freely distributed in the framework of the IPEV/PNRA Project “Routine Meteorological Observation at Station Concordia” — www.climantartide.it.

References

- Bodas-Salcedo, A., Webb, M.J., Bony, S., Chepfer, H., Dufresne, J.L., Klein, S.A., Zhang, Y., Marchand, R., Haynes, J.M., Pincus, R., John, V.O., 2011. COSP: Satellite simulation software for model assessment. *Bull. Amer. Meteor. Soc.* 92, 1023–1043. doi:10.1175/2011bams2856.1.
- Bonne, J.L., Masson-Delmotte, V., Cattani, O., Delmotte, M., Risi, C., Sodemann, H., Steen-Larsen, H.C., 2014. The isotopic composition of water vapour and precipitation in Ivittuut, southern Greenland. *Atmos. Chem. Phys.* 14, 4419–4439. doi:10.5194/acp-14-4419-2014.
- Bonne, J.L., Steen-Larsen, H.C., Risi, C., Werner, M., Sodemann, H., Lacour, J.L., Fettweis, X., Cesana, G., Delmotte, M., Cattani, O., Vallerlonga, P., Kjær, H.A., Clerbaux, C., Sveinbjörnsdóttir, Á.E., Masson-Delmotte, V., 2015. The summer 2012 Greenland heat wave: In situ and remote sensing observations of water vapor isotopic composition during an atmospheric river event. *J. Geophys. Res. Atmos.* 120, 2970–2989. doi:10.1002/2014JD022602.
- Braconnot, P., Harrison, S.P., Kageyama, M., Bartlein, P.J., Masson-Delmotte, V., Abe-Ouchi, A., Otto-Bliesner, B., Zhao, Y., 2012. Evaluation of climate models using palaeoclimatic data. *Nat. Clim. Change* 2, 417–424. doi:10.1038/nclimate1456.
- Brook, E.J., White, J.W.C., Schilla, A.S.M., Bender, M.L., Barnett, B., Severinghaus, J.P., Taylor, K.C., Alley, R.B., Steig, E.J., 2005. Timing of millennial-scale climate change at Siple Dome, West Antarctica, during the last glacial period. *Quat. Sci. Rev.* 24, 1333–1343. doi:10.1016/j.quascirev.2005.02.002.
- Casado, M., Ortega, P., Masson-Delmotte, V., Risi, C., Swingedouw, D., Daux, V., Genty, D., Maignan, F., Solomina, O., Vinther, B., Viovy, N., Yiou, P., 2013. Impact of precipitation intermittency on NAO-temperature signals in proxy records. *Clim. Past* 9, 871–886. doi:10.5194/cp-9-871-2013.
- Cauquoin, A., Jean-Baptiste, P., Risi, C., Fourré, É., Landais, A., 2016. Modeling the global bomb tritium transient signal with the AGCM LMDZ-iso: A method to evaluate aspects of the hydrological cycle. *J. Geophys. Res. Atmos.* 121, 12,612–12,629. doi:10.1002/2016JD025484.
- Cesana, G., Chepfer, H., 2012. How well do climate models simulate cloud vertical structure? A comparison between CALIPSO-GOCCP satellite observations and CMIP5 models. *Geophys. Res. Lett.* 39, 20803. doi:10.1029/2012GL053153.
- Chepfer, H., Bony, S., Winker, D., Cesana, G., Dufresne, J.L., Minnis, P., Stubenrauch, C.J., Zeng, S., 2010. The GCM-Oriented CALIPSO Cloud Product (CALIPSO-GOCCP). *J. Geophys. Res.* 115. doi:10.1029/2009jd012251.
- Compo, G.P., Whitaker, J.S., Sardeshmukh, P.D., Matsui, N., Allan, R.J., Yin, X., Gleason, B.E., Vose, R.S., Rutledge, G., Bessemoulin, P., Brönnimann, S., Brunet, M., Crouthamel, R.I., Grant, A.N., Groisman, P.Y., Jones, P.D., Kruk, M.C., Kruger, A.C., Marshall, G.J., Maugeri, M., Mok, H.Y., Nordli, Ø., Ross, T.F., Trigo, R.M., Wang, X.L., Woodruff, S.D., Worley, S.J., 2011. The Twentieth Century Reanalysis Project. *Quart. J. Roy. Meteor. Soc.* 137, 1–28. doi:10.1002/qj.776.
- EPICA Comm. Members, 2004. Eight glacial cycles from an Antarctic ice core. *Nature* 429, 623–628. doi:10.1038/nature02599.
- Galewsky, J., Hurley, J.V., 2010. An advection-condensation model for subtropical water vapor isotopic ratios. *J. Geophys. Res.* 115, D16116. doi:10.1029/2009jd013651.
- Gates, W.L., 1992. AMIP: The Atmospheric Model Intercomparison Project. *Bull. Am. Meteorol. Soc.* 73, 1962–1970. doi:10.1175/1520-0477(1992)073<1962:atamip>2.0.co;2.
- Godunov, S.K., 1959. Finite-difference methods for the numerical computations of equations of gas dynamics. *Math. Sb.* 7, 271–290.
- Hendricks, M.B., DePaolo, D.J., Cohen, R.C., 2000. Space and time variation of $\delta^{18}\text{O}$ and δD in precipitation: Can paleotemperature be estimated from ice cores? *Global Biogeochem. Cycles* 14, 851–861. doi:10.1029/1999gb001198.
- Hourdin, F., Armengaud, A., 1999. The Use of Finite-Volume Methods for Atmospheric Advection of Trace Species. Part I: Test of Various Formulations in a General Circulation Model. *Mon. Weather Rev.* 127, 822–837. doi:10.1175/1520-0493(1999)127<0822:tuofvm>2.0.co;2.
- Hourdin, F., Foujols, M.A., Codron, F., Guemas, V., Dufresne, J.L., Bony, S., Denvil, S., Guez, L., Lott, F., Ghattas, J., Braconnot, P., Marti, O., Meurdesoif, Y., Bopp, L., 2013. Impact of the LMDZ atmospheric grid configuration on the climate and sensitivity of the IPSL-CM5A coupled model. *Clim. Dynam.* 40, 2167–2192. doi:10.1007/s00382-012-1411-3.
- Hourdin, F., Musat, I., Bony, S., Braconnot, P., Codron, F., Dufresne, J.L., Fairhead, L., Filiberti, M.A., Friedlingstein, P., Grandpeix, J.Y., Krinner, G., LeVan, P., Li, Z.X., Lott, F., 2006. The LMDZ4 general circulation model: climate performance and sensitivity to parametrized physics with emphasis on tropical convection. *Clim. Dynam.* 27, 787–813. doi:10.1007/s00382-006-0158-0.
- Joussaume, S., Sadourny, R., Jouzel, J., 1984. A general circulation model of water isotope cycles in the atmosphere. *Nature* 311, 24–29. doi:10.1038/311024a0.
- Jouzel, J., 2013. A brief history of ice core science over the last 50 yr. *Clim. Past* 9, 2525–2547. doi:10.5194/cp-9-2525-2013.
- Jouzel, J., Masson-Delmotte, V., Cattani, O., Dreyfus, G., Falourd, S., Hoffmann, G., Minster, B., Nouet, J., Barnola, J.M., Blunier, T., Chappellaz, J., Fischer, H., Gallet, J.C., Johnsen, S., Leuenberger, M., Loulergue, L., Luethi, D., Oerter, H., Parrenin, F., Raisbeck, G., Raynaud, D., Schilt, A., Schwander, J., Delmo, E., Souchez, R., Spahni, R., Stauffer, B., Steffensen, J.P., Stenni, B., Stocker, T.F., Tison, J.L., Werner, M., Wolff, E., 2007. Orbital and Millennial Antarctic Climate Variabil-

- ity over the Past 800,000 Years. *Science* 317, 793–796. doi:10.1126/science.1141038.
- Krinner, G., Genthon, C., Li, Z.X., Le Van, P., 1997. Studies of the Antarctic climate with a stretched-grid general circulation model. *J. Geophys. Res. Atmos.* 102, 13731–13745. doi:10.1029/96JD03356.
- Lacour, A., Chepfer, H., Miller, N.B., Shupe, M.D., Noel, V., Fettweis, X., Gallee, H., Kay, J.E., Guzman, R., Cole, J., 2018. How Well Are Clouds Simulated over Greenland in Climate Models? Consequences for the Surface Cloud Radiative Effect over the Ice Sheet. *J. Climate* 31, 9293–9312. doi:10.1175/jcli-d-18-0023.1.
- Landais, A., Barkan, E., Luz, B., 2008. Record of $\delta^{18}\text{O}$ and ^{17}O -excess in ice from Vostok Antarctica during the last 150,000 years. *Geophys. Res. Lett.* 35, 2709. doi:10.1029/2007GL032096.
- Landais, A., Ekaykin, A., Barkan, E., Winkler, R., Luz, B., 2012. Seasonal variations of ^{17}O -excess and d-excess in snow precipitation at Vostok station, East Antarctica. *J. Glaciol.* 58, 725–733. doi:10.3189/2012jog11j237.
- Lee, J.E., Fung, I., Depaolo, D.J., Henning, C.C., 2007. Analysis of the global distribution of water isotopes using the NCAR atmospheric general circulation model. *J. Geophys. Res.* 112, 16306. doi:10.1029/2006JD007657.
- van Leer, B., 1977. Towards the ultimate conservative difference scheme. IV. A new approach to numerical convection. *J. Comput. Phys.* 23, 276–299. doi:10.1016/0021-9991(77)90095-x.
- Lott, F., Fairhead, L., Hourdin, F., LeVan, P., 2005. The stratospheric version of LMDz: dynamical climatologies, arctic oscillation, and impact on the surface climate. *Clim. Dynam.* 25, 851–868. doi:10.1007/s00382-005-0064-x.
- Marti, O., Braconnot, P., Bellier, J., Benshila, R., Bony, S., Brockmann, P., Cadule, P., Caubel, A., Denvil, S., Dufresne, J.L., Fairhead, L., Filiberti, M.A., Fichet, T., Foujols, M.A., Friedlingstein, P., Grandpeix, J.Y., Hourdin, F., Krinner, G., Lévy, C., Madec, G., Musat, I., De Noblet, N., Polcher, J., Talandier, C., 2005. The new IPSL climate system model: IPSL-CM4. Tech Report 26. IPSL. URL: <https://hal-insu.archives-ouvertes.fr/insu-00421338>.
- Masson-Delmotte, V., Hou, S., Ekaykin, A., Jouzel, J., Aristarain, A., Bernardo, R.T., Bromwich, D., Cattani, O., Delmotte, M., Falourd, S., Frezzotti, M., Gallée, H., Genoni, L., Isaksson, E., Landais, A., Helsen, M., Hoffmann, G., Lopez, J., Morgan, V., Motoyama, H., Noone, D., Oerter, H., Petit, J.R., Royer, A., Uemura, R., Schmidt, G.A., Schlosser, E., Simões, J.C., Steig, E., Stenni, B., Stievenard, M., van den Broeke, M., van de Wal, R., van de Berg, W.J., Vimeux, F., White, J.W.C., 2008. A review of Antarctic surface snow isotopic composition: observations, atmospheric circulation and isotopic modelling. *J. Climate* 21, 3359–3387. doi:10.1175/2007JCLI2139.1.
- Masson-Delmotte, V., Kageyama, M., Braconnot, P., Charbit, S., Krinner, G., Ritz, C., Guilyardi, E., Jouzel, J., Abe-Ouchi, A., Crucifix, M., Gladstone, R.M., Hewitt, C.D., Kitoh, A., LeGrande, A.N., Marti, O., Merkel, U., Motoi, T., Ohgaito, R., Otto-Bliesner, B., Peltier, W.R., Ross, I., Valdes, P.J., Vettoretti, G., Weber, S.L., Wolk, F., Yu, Y., 2006. Past and future polar amplification of climate change: climate model intercomparisons and ice-core constraints. *Clim. Dynam.* 26, 513–529. doi:10.1007/s00382-005-0081-9.
- Peltier, W.R., 1994. Ice Age Paleotopography. *Science* 265, 195–201. doi:10.1126/science.265.5169.195.
- Risi, C., Bony, S., Vimeux, F., Jouzel, J., 2010a. Correction to “Water-stable isotopes in the LMDZ4 general circulation model: Model evaluation for present-day and past climates and applications to climatic interpretations of tropical isotopic records”. *J. Geophys. Res. Atmos.* 115. doi:10.1029/2010jd015242.
- Risi, C., Bony, S., Vimeux, F., Jouzel, J., 2010b. Water-stable isotopes in the LMDZ4 general circulation model: Model evaluation for present-day and past climates and applications to climatic interpretations of tropical isotopic records. *J. Geophys. Res. Atmos.* 115, 12118. doi:10.1029/2009JD013255.
- Risi, C., Landais, A., Winkler, R., Vimeux, F., 2013. Can we determine what controls the spatio-temporal distribution of d-excess and ^{17}O -excess in precipitation using the LMDZ general circulation model? *Clim. Past* 9, 2173–2193. doi:10.5194/cp-9-2173-2013.
- Risi, C., Noone, D., Worden, J., Frankenberg, C., Stiller, G., Kiefer, M., Funke, B., Walker, K., Bernath, P., Schneider, M., Bony, S., Lee, J., Brown, D., Sturm, C., 2012. Process-evaluation of tropospheric humidity simulated by general circulation models using water vapor isotopic observations: 2. Using isotopic diagnostics to understand the mid and upper tropospheric moist bias in the tropics and subtropics. *J. Geophys. Res. Atmos.* 117, 5304. doi:10.1029/2011JD016623.
- Ritter, F., Steen-Larsen, H.C., Werner, M., Masson-Delmotte, V., Orsi, A., Behrens, M., Birnbaum, G., Freitag, J., Risi, C., Kipfstuhl, S., 2016. Isotopic exchange on the diurnal scale between near-surface snow and lower atmospheric water vapor at Kohnen station, East Antarctica. *The Cryosphere* 10, 1647–1663. doi:10.5194/tc-10-1647-2016.
- Schoenemann, S.W., Steig, E.J., Ding, Q., Markle, B.R., Schauer, A.J., 2014. Triple water-isotopologue record from WAIS Divide, Antarctica: Controls on glacial-interglacial changes in $^{17}\text{O}_{\text{excess}}$ of precipitation. *J. Geophys. Res. Atmos.* 119, 8741–8763. doi:10.1002/2014jd021770.
- Steen-Larsen, H.C., Johnsen, S.J., Masson-Delmotte, V., Stenni, B., Risi, C., Sodemann, H., Balslev-Clausen, D., Blunier, T., Dahl-Jensen, D., Ellehøj, M.D., Falourd, S., Grindsted, A., Gkinis, V., Jouzel, J., Popp, T., Sheldon, S., Simonsen, S.B., Sjolte, J., Steffensen, J.P., Sperlich, P., Sveinbjörnsdóttir, A.E., Vinther, B.M., White, J.W.C., 2013. Continuous monitoring of summer surface water vapor isotopic composition above the Greenland Ice Sheet. *Atmos. Chem. Phys.* 13, 4815–4828. doi:10.5194/acp-13-4815-2013.
- Steen-Larsen, H.C., Masson-Delmotte, V., Hirabayashi, M., Winkler, R., Satow, K., Prié, F., Bayou, N., Brun, E., Cuffey, K.M., Dahl-Jensen, D., Dumont, M., Guillemin, M., Kipfstuhl, S., Landais, A., Popp, T., Risi, C., Steffen, K., Stenni, B., Sveinbjörnsdóttir, A.E., 2014. What controls the isotopic composition of Greenland surface snow? *Clim. Past* 10, 377–392. doi:10.5194/cp-10-377-2014.
- Steen-Larsen, H.C., Risi, C., Werner, M., Yoshimura, K., Masson-Delmotte, V., 2017. Evaluating the skills of isotope-enabled general circulation models against in situ atmospheric water vapor isotope observations. *J. Geophys. Res. Atmos.* 122, 246–263. doi:10.1002/2016jd025443.
- Stenni, B., Masson-Delmotte, V., Selmo, E., Oerter, H., Meyer, H., Röthlisberger, R., Jouzel, J., Cattani, O.,

- Falourd, S., Fischer, H., Hoffmann, G., Iacumin, P., Johnsen, S.J., Minster, B., Udisti, R., 2010. The deuterium excess records of EPICA Dome C and Dronning Maud Land ice cores (East Antarctica). *Quat. Sci. Rev.* 29, 146–159. doi:10.1016/j.quascirev.2009.10.009.
- Stenni, B., Scarchilli, C., Masson-Delmotte, V., Schlosser, E., Ciardini, V., Dreossi, G., Grigioni, P., Bonazza, M., Cagnati, A., Karlicek, D., Risi, C., Udisti, R., Valt, M., 2016. Three-year monitoring of stable isotopes of precipitation at Concordia Station, East Antarctica. *The Cryosphere* 10, 2415–2428. doi:10.5194/tc-10-2415-2016.
- Touzeau, A., Landais, A., Stenni, B., Uemura, R., Fukui, K., Fujita, S., Guilbaud, S., Ekaykin, A., Casado, M., Barkan, E., Luz, B., Magand, O., Teste, G., Le Meur, E., Baroni, M., Savarino, J., Bourgeois, I., Risi, C., 2016. Acquisition of isotopic composition for surface snow in East Antarctica and the links to climatic parameters. *The Cryosphere* 10, 837–852. doi:10.5194/tc-10-837-2016.
- Vignon, É., Hourdin, F., Genthon, C., Gallée, H., Bazile, É., Lefebvre, M.P., Madeleine, J.B., Van de Wiel, B.J.H., 2017. Antarctic boundary layer parametrization in a general circulation model: 1-D simulations facing summer observations at Dome C. *J. Geophys. Res. Atmos.* 122, 6818–6843. doi:10.1002/2017jd026802.
- Vignon, É., Hourdin, F., Genthon, C., Van de Wiel, B.J.H., Gallée, H., Madeleine, J.B., Beaumet, J., 2018. Modeling the Dynamics of the Atmospheric Boundary Layer Over the Antarctic Plateau With a General Circulation Model. *J. Adv. Model. Earth Syst.* 10, 98–125. doi:10.1002/2017ms001184.
- Vimeux, F., Masson, V., Delaygue, G., Jouzel, J., Petit, J.R., Stievenard, M., 2001. A 420,000 year deuterium excess record from East Antarctica: Information on past changes in the origin of precipitation at Vostok. *J. Geophys. Res. Atmos.* 106, 31863–31873. doi:10.1029/2001jd900076.
- WAIS Divide Project Members, 2013. Onset of deglacial warming in West Antarctica driven by local orbital forcing. *Nature* 500, 440–444. doi:10.1038/nature12376.
- Werner, M., Heimann, M., Hoffmann, G., 2001. Isotopic composition and origin of polar precipitation in present and glacial climate simulations. *Tellus B* 53, 53–71. doi:10.3402/tellusb.v53i1.16539.
- Werner, M., Langebroek, P.M., Carlsen, T., Herold, M., Lohmann, G., 2011. Stable water isotopes in the ECHAM5 general circulation model: Toward high-resolution isotope modeling on a global scale. *J. Geophys. Res. Atmos.* 116, 15109. doi:10.1029/2011JD015681.